geoconvention
Calgary • Canada • May 11-13 2026

Reconstruction of Poisson Disk–Sampled Seismic Data using Compressive Sensing

Prateek Nandi and Mauricio D. Sacchi

Signal Analysis and Imaging Group (SAIG), Department of Physics, University of Alberta

Summary

We present a reconstruction algorithm for 3D seismic datasets based on compressive sensing (CS) using Poisson disk sampling (PDS) in the spatial domain. Poisson disk sampling enforces a minimum separation distance between sample locations, producing a quasi-uniform distribution with blue-noise characteristics. This reduces both clustering and significant unsampled gaps, which can negatively impact reconstruction quality.

In this work, Poisson disk sampling is used strictly as a geometric sampling strategy to define the sensing operator. Its performance is compared with uniform random and jittered undersampling using a real seismic dataset that is deliberately decimated to simulate a common-offset 3D volume. Reconstruction quality is evaluated using signal-to-noise ratio (SNR) as a function of sampling density. The results demonstrate that Poisson disk sampling consistently yields higher SNR than the alternative sampling strategies over a wide range of decimation factors.

Introduction

Seismic acquisition is often constrained by logistical, environmental, and economic factors, leading to incomplete or irregular spatial sampling. Classical acquisition design typically follows the Nyquist–Shannon sampling theorem, which guarantees alias-free sampling on uniform grids but leads to dense acquisition requirements that are frequently impractical for large 3D surveys.

To address incomplete sampling, several reconstruction approaches have been developed. Prediction-error filters (PEF) exploit spatial predictability to interpolate missing traces [Spitz, 1991]. Transform-based methods rely on sparsity in domains such as Fourier or curvelets to reconstruct missing or aliased data [Sacchi et al., 1998, Herrmann et al., 2008].

Compressive sensing (CS) provides a framework for recovering signals from fewer samples than those required by uniform Nyquist–Shannon sampling, provided that the signal is sparse in a suitable transform domain and that the sampling operator exhibits sufficient incoherence [Herrmann, 2010]. In this context, the spatial sampling pattern plays a critical role.

Poisson disk sampling (PDS), initially developed in computer graphics, generates randomized sample distributions subject to a minimum-distance constraint [Bridson, 2007]. The resulting blue-noise spectra avoid strong periodicity while maintaining uniform coverage, properties that are desirable for CS-based reconstruction. This work investigates the impact of Poisson disk sampling on seismic data reconstruction and compares it with jittered and uniform random undersampling strategies.

Theory

The observed irregularly sampled seismic data $\mathbf{d}$ are modelled as

$$\mathbf{d} = \mathcal{S}\,\mathbf{m}, \tag{1}$$

where $\mathcal{S}$ denotes the sampling operator and $\mathbf{m}$ is the fully sampled seismic signal. For instance, $\mathbf{d}$ can denote a constant-offset cube that depends on inline and crossline CMP coordinates and time, where not all spatial positions are recorded. The objective is to recover the fully populated cube $\mathbf{m}$ corresponding to the data one would ideally acquire on a regular grid.

We assume that $\mathbf{m}$ admits a sparse representation in the Fourier domain:

$$\mathbf{m} = \mathcal{F}^H \boldsymbol{\alpha}, \tag{2}$$

where $\mathcal{F}^H$ denotes the inverse Fourier transform and $\boldsymbol{\alpha}$ contains the Fourier coefficients indexed by temporal frequency and inline/crossline wavenumbers. Combining the above expressions yields the underdetermined linear system

$$\mathbf{d} = \mathcal{S}\mathcal{F}^H \boldsymbol{\alpha}. \tag{3}$$

Since the number of acquired measurements is smaller than the number of unknowns, this system admits infinitely many solutions due to the nontrivial null space of $\mathcal{S}\mathcal{F}^H$. Consequently, additional constraints are required to select a meaningful solution.

Compressive sensing addresses this indeterminacy by promoting sparsity of the solution in a suitable transform domain [Donoho, 2006]. Specifically, among all solutions that satisfy the data constraints, one seeks the sparsest coefficient vector $\boldsymbol{\alpha}$. Under appropriate conditions on the sensing operator—most notably sufficient incoherence between the sampling operator $\mathcal{S}$ and the sparsifying transform $\mathcal{F}^H$—it can be shown that the sparsest solution can recover the true underlying signal with high probability [Candès et al., 2006].

Hence, the reconstruction problem can be posed as

$$\hat{\boldsymbol{\alpha}} = \arg\min_{\boldsymbol{\alpha}} \ \|\boldsymbol{\alpha}\|_1 \quad \text{subject to} \quad \mathcal{S}\mathcal{F}^H \boldsymbol{\alpha} = \mathbf{d}, \tag{4}$$

and the recovered seismic data are obtained as

$$\hat{\mathbf{m}} = \mathcal{F}^H \hat{\boldsymbol{\alpha}}. \tag{5}$$

The constrained formulation above assumes noise-free observations and therefore requires the sampled data to be matched precisely. In practice, the measurements contain noise. In addition, the synthesis operator $\mathcal{F}^H$ may not provide a perfectly sparse representation of the data for the chosen transform, so an exact fit may force the solution to explain noise and representation mismatch by introducing spurious Fourier coefficients. Therefore, we replace the equality constraint with a least-squares data misfit term and solve the unconstrained (LASSO/BPDN-type) problem [Tibshirani, 1997], enforcing sparsity while allowing controlled mismatch to the observations. Therefore, we solve the unconstrained problem

$$\hat{\boldsymbol{\alpha}} = \arg\min_{\boldsymbol{\alpha}} \ \|\mathbf{d} - \mathcal{S}\mathcal{F}^H \boldsymbol{\alpha}\|_2^2 + \mu \|\boldsymbol{\alpha}\|_1, \tag{6}$$

where μ is used to balance sparsity in the transform coefficients versus data fit level. The optimization is carried out using the Fast Iterative Soft Thresholding Algorithm (FISTA) [Beck and Teboulle, 2009], and the reconstructed data are given by $\hat{\mathbf{m}} = \mathcal{F}^H \hat{\boldsymbol{\alpha}}$.

Sampling Strategies

Three undersampling strategies are considered:

(1) Poisson disk sampling (PDS): A geometric sampling strategy enforcing a minimum distance between sample locations, resulting in quasi-uniform spatial coverage with blue-noise characteristics.

(2) Jittered undersampling: Samples are taken from a coarse regular grid and randomly perturbed within local neighbourhoods, balancing structure and randomness [Hennenfent and Herrmann, 2008].

(3) Uniform random undersampling: Samples are selected independently with equal probability from a regular grid, providing global incoherence but allowing large unsampled gaps.

Poisson Disk Sampling

Poisson disk sampling generates a set of points

$$X = \{(x_i, y_i)\}_{i=1}^{N}$$

within a spatial domain $D \subset \mathbb{R}^2$ such that

$$\|(x_i, y_i) - (x_j, y_j)\| \geq r, \quad \forall i \neq j,$$

where r is a prescribed minimum separation distance. Apart from this constraint, sample locations are random, leading to quasi-uniform spatial distributions without clustering.

In this work, Poisson disk sampling is used solely to define the spatial sampling geometry. The continuous sample coordinates are projected onto the nearest grid locations to construct a binary sampling operator that acts uniformly across time.

Table 1: Poisson Disk Sampling Algorithm for Generating the Sampling Matrix

Item	**Description**
Input	Spatial grid dimensions (N_x, N_y), decimation factor δ, candidate count k (typically 20–30).
Output	Binary sampling matrix $\mathbf{S} \in \mathbb{R}^{N_t \times N_x \times N_y}$.
Steps	**Description**
Step 0	Compute $N_{\text{total}} = N_x N_y$ and target count $N_{\text{target}} = \delta N_{\text{total}}$. Choose radius $r = \sqrt{\frac{2N_x N_y}{\pi N_{\text{target}}}}$, which controls the expected sampling density.
Step 1	Partition the domain into a coarse grid with cell size $r/\sqrt{2}$, restricting distance checks to neighbouring cells.
Step 2	Randomly select an initial sample point (x_0, y_0) and add it to the active list and the sample set $\mathcal{P}$.
Step 3	While the active list is non-empty, randomly select an active point (p_x, p_y).
Step 4	Generate up to k candidate points uniformly in the annulus $[r, 2r]$ centered at (p_x, p_y). Accept a candidate if it lies in the domain and satisfies the minimum-distance constraint to all points in $\mathcal{P}$. Accepted candidates are added to $\mathcal{P}$ and the active list. If no candidate is accepted after k trials, remove (p_x, p_y) from the active list.
Step 5	If $\lvert\mathcal{P}\rvert > N_{\text{target}}$, randomly discard excess points to match the desired sampling fraction.
Step 6	Initialize $\mathbf{S}$ with zeros. For each $(x_i, y_i) \in \mathcal{P}$, project to grid indices $i_x = 1 + \text{round}[(x_i - x_{min})/\Delta x] \quad i_y = 1 + \text{round}[(y_i - y_{min})/\Delta y]$, and set $S(t, i_x, i_y) = 1$ for all $t = 1, \ldots, N_t$.
Step 7	Return $\mathbf{S}$.

Results

The reconstruction performance was evaluated using a real 3D seismic dataset. Figure 1 shows representative examples of decimated data and reconstructed volumes for the three sampling strategies at 30% sampling.

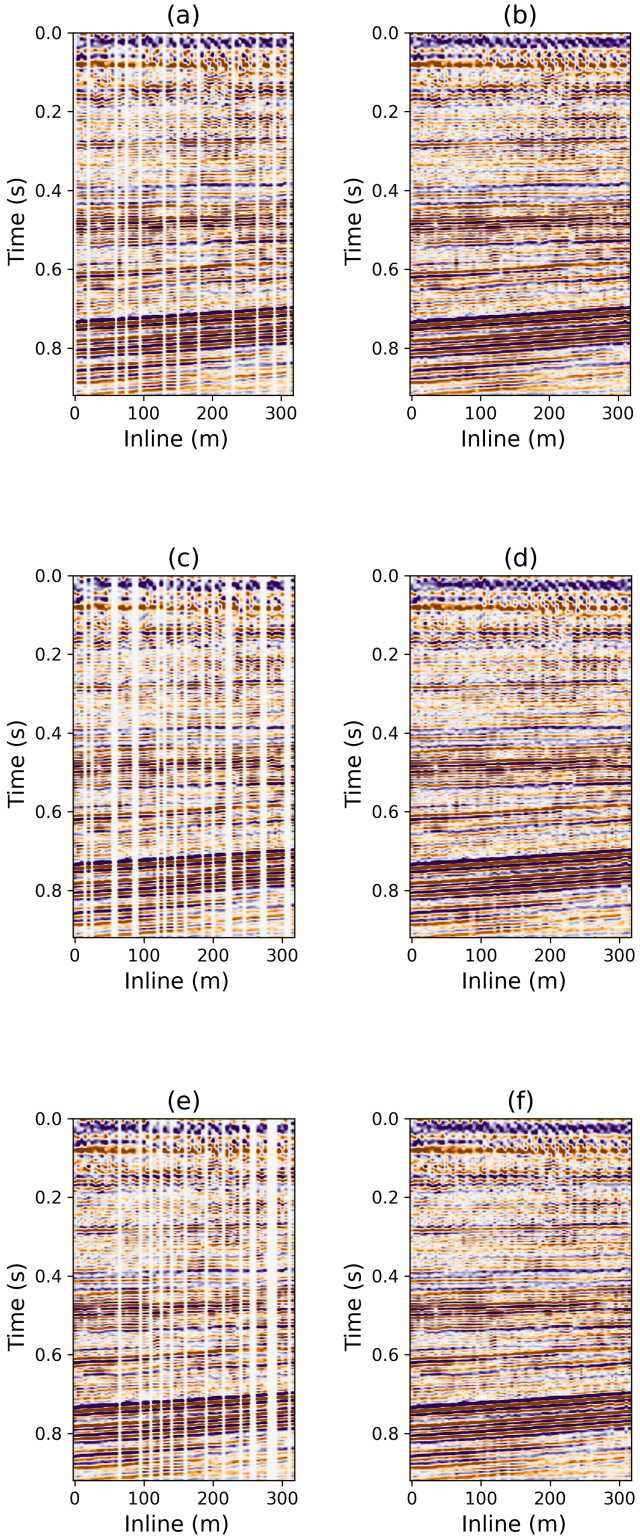


Figure 1: (a) Poisson-disk sampling with 30% decimation (b) Reconstruction from Poisson-disk–sampled data (c) Jittered sampling with 30% decimation (d) Reconstruction from jittered-sampled data (e) Random sampling with 30% decimation (f) Reconstruction from randomly sampled data

Reconstruction quality is quantified using the signal-to-noise ratio

$$\mathrm{SNR} = 20 \log_{10} \frac{\|\mathbf{d}_{\mathsf{true}}\|_2}{\|\mathbf{d}_{\mathsf{true}} - \mathbf{d}_{\mathsf{rec}}\|_2}.$$

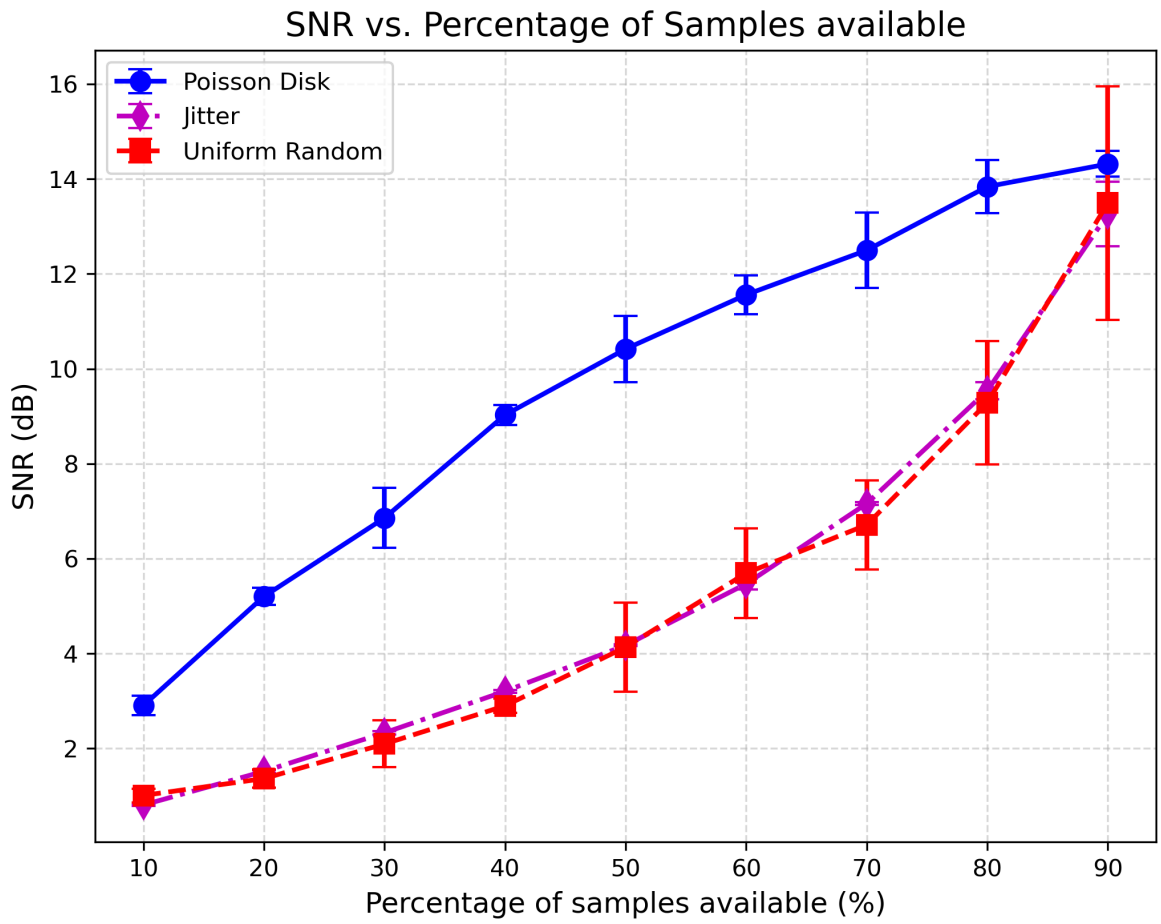


Figure 2: SNR versus sampling percentage for different undersampling strategies. Error bars indicate variance over multiple realizations.

Poisson disk sampling consistently yields higher SNR across all sampling densities (Figure 2). As sampling decreases, all methods exhibit degradation; however, Poisson disk sampling maintains more stable performance due to its uniform spatial coverage and reduced occurrence of large gaps.

Conclusion

The results demonstrate that Poisson disk sampling provides a robust spatial sampling strategy for compressive sensing-based seismic reconstruction. By enforcing a minimum-distance constraint, Poisson disk sampling avoids clustering and large unsampled regions, leading to more stable reconstructions under aggressive decimation. Compared with jittered and uniform random sampling, Poisson disk sampling consistently achieves higher SNR and improved reconstruction quality.

Acknowledgements

We thank the sponsors of the Signal Analysis and Imaging Group (SAIG) at the University of Alberta for their support of this research. We also thank Joaquín Acedo for insightful advice on compressed sensing and for helping to shape the initial direction of this work.

References

[Beck and Teboulle, 2009] Beck, A. and Teboulle, M. (2009). A fast iterative shrinkage-thresholding algorithm for linear inverse problems. *SIAM Journal on Imaging Sciences*, 2(1):183–202.

[Bridson, 2007] Bridson, R. (2007). Fast poisson disk sampling in arbitrary dimensions. *SIGGRAPH sketches*, 10(1):1.

[Candès et al., 2006] Candès, E. J., Romberg, J. K., and Tao, T. (2006). Stable signal recovery from incomplete and inaccurate measurements. *Communications on Pure and Applied Mathematics*, 59(8):1207–1223.

[Donoho, 2006] Donoho, D. (2006). Compressed sensing. *IEEE Transactions on Information Theory*, 52(4):1289–1306.

[Hennenfent and Herrmann, 2008] Hennenfent, G. and Herrmann, F. J. (2008). Simply denoise: Wavefield reconstruction via jittered undersampling. *Geophysics*, 73(3):V19–V28.

[Herrmann, 2010] Herrmann, F. J. (2010). Randomized sampling and sparsity: Getting more information from fewer samples. *Geophysics*, 75(6):WB173–WB187.

[Herrmann et al., 2008] Herrmann, F. J., Wang, D., Hennenfent, G., and Moghaddam, P. P. (2008). Curvelet-based seismic data processing: A multiscale and nonlinear approach. *Geophysics*, 73(1):A1–A5.

[Sacchi et al., 1998] Sacchi, M. D., Ulrych, T. J., and Walker, C. J. (1998). Interpolation and extrapolation using a high-resolution discrete fourier transform. *IEEE Transactions on Signal Processing*, 46(1):31–38.

[Spitz, 1991] Spitz, S. (1991). Seismic trace interpolation in the *F-X* domain. *Geophysics*, 56(6):785–794.

[Tibshirani, 1997] Tibshirani, R. (1997). The lasso method for variable selection in the cox model. *Statistics in Medicine*, 16(4):385–395.